THE ASTROPHYSICAL JOURNAL, 357:531–538, 1990 July 10

THE ^{13}CO–A_V RELATION AT HIGH EXTINCTIONS: THE ρ OPHIUCHI COMPLEX

ROBERT L. DICKMAN
Department of Physics and Astronomy, University of Massachusetts at Amherst
AND
WILLIAM HERBST
Van Vleck Observatory, Wesleyan University
Received 1989 August 10; accepted 1990 January 15

ABSTRACT

We have carried out a study of the ^{13}CO–A_V relation at high visual extinctions in a $40' \times 40'$ section of the ρ Oph molecular cloud complex. The molecular data consist of LTE column density maps based on $J = 1 \rightarrow 0$ CO and ^{13}CO observations made with the 14 m FCRAO radio telescope. The optical data are derived from star counts at $\lambda \sim 8000$ Å made from deep, wide-field photographic plates obtained with the Cerro Tololo 4 m telescope. By establishing our own calibrated stellar surface density curves, we avoid many of the difficulties associated with using star counts to determine very high extinctions.

LTE ^{13}CO column density is found to be well correlated with visual extinction on spatial scales of $\sim 3'$ in the range $0 \leq A_V \leq 10$ mag. A least-squares fit gives the result

$$N_{13}^{\rm fit} = (2.16 \pm 0.12)A_V - (3.06 \pm 0.90) ,$$

where $N_{13}^{\rm fit}$ is in units of 10^{15} cm^{-2}.

The slope of this relation is consistent with our own and other previous work except in the case of the Taurus clouds, where a significantly lower slope has been found. The nonzero intercept in the relation above indicates that there is an extinction threshold of 1.4 mag in the ρ Oph clouds which must be exceeded in order for there to be observable ^{13}CO emission. We argue that the threshold is produced by a diffuse, foreground layer of the main Ophiuchus cloud, in which densities are too low, and photodissociation processes too strong to permit significant carbon monoxide formation. As such, the *molecular* mass of the ρ Oph clouds should be well established by simply using the *slope* of the relation above and ignoring the offset entirely. However, envelopes considerably denser than that of the Oph cloud are likely to be common and precautions should therefore be taken to account for their potential contribution to molecular cloud masses.

Subject headings: interstellar: molecules — nebulae: individual (ρ Oph)

I. INTRODUCTION

Molecular hydrogen, the main constituent of molecular clouds, is essentially unobservable from the surface of the Earth except in shock-excited or fluorescent regions. Not only is the molecule so light that its rotational transitions lie in the mid-infrared where atmospheric transmission is extremely poor, but its lack of a permanent electric dipole moment means that its pure rotational lines are inherently very weak. While H_2 u-v absorption lines can be detected in the spectra of early-type stars lying at the edges of some clouds, as a general matter these facts have forced astronomers to rely upon indirect methods to estimate molecular cloud masses and internal mass distributions. One such method involves the use of secondary tracers: easily-observed cloud constituents that can be shown to correlate with less easily studied species themselves known or believed to securely reflect H_2 mass (Dickman 1988).

Beginning with the pioneering work of Encrenaz, Falgarone, and Lucas (1975), carbon monoxide has become the most commonly used of these secondary tracers. There are a number of reasons for this. CO and its less abundant isotopic variants are widespread in the interstellar medium and the molecule's low permanent dipole moment renders it easily excited by collisions with H_2. In addition, the molecule's lowest rotational transition lies at $\lambda = 2.6$ mm and is thus easily observed at high spatial resolution. Moreover, since the work of Lilley (1955), visual extinction, A_V, has been known to be a remarkably reliable tracer of proton column density, at least at low extinctions (Bohlin, Savage, and Drake 1978), and numerous studies have established that in local molecular clouds, LTE column densities of the rare carbon monoxide species ^{13}CO and C^{18}O correlate in an approximately linear fashion with A_V up to ~ 5–6 mag (e.g., Encrenaz, Falgarone, and Lucas 1975; Tucker *et al.* 1976; Dickman 1978*a*; Elmegreen and Elmegreen 1979; Frerking, Langer, and Wilson 1982; Dickman and Clemens 1983; Duvert, Cernicharo, and Baudry 1986; Bachiller and Cernicharo 1986; Cernicharo and Güelin 1987; see summary by Bachiller and Cernicharo 1986).

However, with the exception of the work by Frerking, Langer, and Wilson (1982; hereafter FLW), none of the studies cited above involve *measured* visual extinctions greater than ~ 4–6 mag (as opposed to lower limits). Extinctions above these limits are of particular interest, since they offer the potential to probe mass distributions within the dense molecular cores which ultimately produce stars.

FLW studied the relation between ^{13}CO column density and visual extinction in the nearby Taurus and ρ Ophiuchi dark cloud complexes; the C^{18}O–A_V relation was also investigated. While the slopes of the N_{13} versus A_V relations found by FLW were consistent with those found by other workers up to that point (although they differed between the 2 clouds in a statistically significant manner), FLW also found significant, nonzero intercepts in their correlations, suggesting the pre-

sence of nonzero extinction thresholds below which molecular column densities were not measurable; such intercepts had not been previously noted. Moreover, FLW's work indicated the presence of breaks and/or nonlinearities in the N_{13}–A_V correlations, features which would greatly limit the usefulness of the easily observed ^{13}CO isotopic species as a mass tracer in molecular clouds.

The extinctions which form an important underpinning to FLW's work were not determined as part of their study. Instead, they were taken from Elias' (1978*a*, *b*) infrared surveys of the Ophiuchus and Taurus clouds. In that work, Elias attempted to distinguish heavily obscured background stars (usually late-type giants) from embedded IR sources by using CO bandhead strengths as a criterion for spectral classification. Multicolor IR photometry then yielded an estimate of the color excess and thus the extinction suffered by the stars.

Although this technique is a powerful one, its use in connection with FLW's study raises some concerns. First, the stars observed by Elias are all intrinsically quite luminous and thus potentially very distant. This raises the worrisome possibility that part (or all) of the extinctions inferred for the background stars are not associated with the molecular clouds which are the subject of FLW's study, but arise instead from general interstellar reddening. Further, if molecular clouds are strongly clumped on small scales, as has been suggested on both observational (e.g., Matsakis *et al.* 1981; Harris *et al.* 1988; Migenes *et al.* 1990; Taylor 1989) and theoretical (e.g., Kwan and Sanders 1986) grounds, the extinction of the very narrow dust column lying between the star and the Earth may reflect very poorly the average extinction of the area subtended by a typical radio telescope beam. Related to this is the fact that if the clouds studied by Elias are clumpy, the IR survey technique will lead to the preferential selection of columns with usually low extinctions. Finally, not only is Elias' spectral classification of background stars necessarily approximate, but the relation between infrared color excess and extinction is uncertain, since it depends upon the behavior of the IR extinction curve in heavily obscured regions.

All these factors make it desirable to reinvestigate the ^{13}CO–A_V relation in these clouds at high extinctions using a technique different from that of Elias to establish the optical obscurations. In this paper we do so for the ρ Oph cloud by using star counts to determine the visual extinctions; results for the Taurus cloud will be discussed elsewhere. The use of star counts to determine extinctions is well established (Bok and McCarthy 1974; Dickman 1978*b*), but for highly obscured clouds requires the use of deep, red-sensitive materials in order to penetrate the dust. For this purpose, we utilize multicolor, magnitude-calibrated prime focus plates taken with the Cerro Tololo 4 m telescope. Details are provided in the next section, along with a description of the radio data and the methods used to analyze them. In § III, we discuss the resulting ^{13}CO–A_V relation and compare it with previous work for this and other clouds. Section IV summarizes the paper's results and conclusions.

II. DATA GATHERING AND REDUCTION

a) Optical Data

Our optical data consist of prime focus plates in three colors taken with the 4 m CTIO telescope. The field of view of the prime focus camera is circular and $\sim$50′ in diameter. Two fields were observed, one centered on a section of the cloud [$\alpha(1950) = 16^h30^m00^s.0$ $\delta(1950) = -24°30'00''$], the other on a reference field judged to be nearly free of obscuration [$\alpha(1950) = 16^h32^m30^s.0$, $\delta(1950) = -25°00'00''$]. The question of extinction in the reference field is discussed further in § III.

TABLE 1

PROPERTIES OF KRON *J*, *F*, AND *N* BANDS

Band	Emulsion	Filter	λ_0(Å)[a]	$\Delta\lambda$(Å)[a]	(A_V/A_λ)[b]
J	IIIa-J	GG385	4627	487	0.80
F	IIIa-F	GG495	6167	599	1.18
N	IV-N[c]	RG695	7941	562	1.69

[a] Bruzual 1966; Kron 1980.
[b] Savage and Mathis 1979.
[c] Hypered.

Plates were hypered and exposed in the Kron *J*, *F*, and *N* bands whose properties (Bruzual 1966) are summarized in Table 1. The exposures were carried out with a Racine wedge, which produced a secondary image of each star displaced by $\sim$30″ from the primary and $\sim$6.9 mag fainter. The exact magnitude shift is determined from the photometry described below.

The plates were scanned using the Yale PDS. Right ascension and declination coordinates of the stars in the cloud field were established from the positions of two SAO stars, 184414 and 184460, located in the field. In order to calibrate the magnitudes of the stellar images, precise *B*, *V*, *R*, and *I* magnitudes were obtained for a number of stars in both the cloud and reference fields having apparent magnitudes ranging from $\sim$12–17, by using the single-channel RCA C31034A PMT photometer on the 60″ CTIO telescope. After transforming these data to *J*, *F*, and *N*, according to

$$J = B - 0.23(B-V)\,, \quad F = V - 0.40(B-V)\,, \quad N = I$$

(Kron 1980; Fernie 1983), we obtained a trio of calibration curves for the reference stars and their secondary images, relating their PDS machine magnitudes to their photometrically determined *J*, *F*, and *N* magnitudes. The resulting curves were then applied to the PDS data, yielding a catalog of stellar positions and magnitudes at *J*, *F*, and *N*. Figure 1 illustrates the cloud field in the *N* band.

The typical stellar magnitude error is $\sim$0.1–0.2, independent of color, for stars fainter than $\sim$18 mag, with smaller errors for brighter stars. A summary of the limiting magnitude in each color for the cloud and reference fields is provided in Table 2. These limits are highly conservative, in the sense that the plates contain bona fide stellar images 1–2 mag fainter than the tabulated values; however, below the limits given, the accuracy of the stellar brightnesses declines because of signal-to-noise limitations, and the possibility of misidentifying plate flaws and noise as stars increases sharply.

TABLE 2

LIMITING MAGNITUDES OF EXPOSURES

Object	Band	m_{lim}
Cloud	*J*	23.5
Cloud	*F*	22.0
Cloud	*N*	19.5
Reference	*J*	20.0
Reference	*F*	19.0
Reference	*N*	18.0

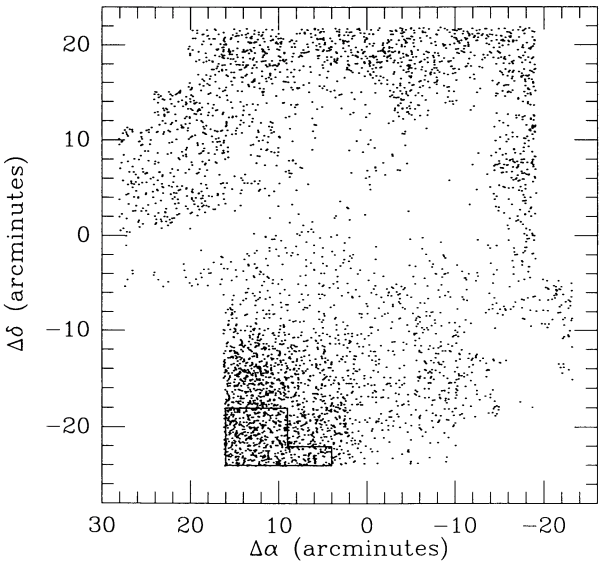

FIG. 1.—The cloud field in the Kron N band (λ_0 = 7941 Å). All stars brighter than apparent magnitude m_N = 19.5 are plotted. Coordinates are offsets in arcminutes from the field center α(1950.0) = 16^{h}30^m, δ(1950.0) = −24°30′. The boxed area in the southeast is the region used to extend the star count sequences beyond the magnitude limits of the reference plate, as described in § II*a*.

In order to determine extinctions, A_λ, in the cloud at a color λ, using star counts, it is necessary to know how the cumulative surface density of stars, $N(m_\lambda)$ varies with apparent magnitude, m_λ, in the absence of obscuration. Ordinarily, one obtains this function directly from the reference field data under the assumption that the field is clear of extinction (if there is a small amount of residual opacity, δA, present, the resulting extinctions are uniformly too great by δA; we discuss this point more fully in § III below).

In the present case, as shown in Table 2, the reference field exposures are ~1–3 mag shallower than those for the cloud field; unless we somehow extend the surface density curves to the limiting magnitudes of the cloud exposures, the zero point of the extinctions will therefore be uncertain. To circumvent this difficulty, we adopt the following procedure. Although there is obscuration everywhere over the cloud plate, the extinction in the SE portion of the cloud field is clearly relatively small, and, more important, as shown by star counts, nearly *uniform* in the area boxed in Figure 1. In Figures 2*a*–2*c*, we show the cumulative stellar surface densities in each color, both for the reference field and the boxed subsection of the cloud field. The densities $N(m_\lambda)$, which give the number of stars brighter than magnitude m_λ have all been normalized to an area of 1 deg^2; the error bars reflect the $\sqrt{n}$ uncertainty associated with a count of n stars (Bok 1937).

The density curves for the small portion of the cloud field are displaced in all three colors from those for the reference field because the boxed field is not completely free of extinction. Under the assumption that the background star density must be the same in both fields (which lie only ~0.°5 apart), we can determine this extinction at each color and adjust the density curves for it. The final curves are shown in Figures 3*a*–3*c*. These were generated by removing extinctions (i.e., offsets in m_λ due to extinction) of $\delta A_J \sim 1.3$ mag, $\delta A_F \sim 1.0$ mag, and $\delta A_N \sim 0.6$ mag. The ratios of these values are governed by the ratio of total to selective extinction (see below) in the lightly obscured portion of the cloud field. The ratio $(\delta A_J/\delta A_F)$ implies a value R = 4, but the ratio $(\delta A_F/\delta A_N)$ implies a "standard" value R ~ 3 (Savage and Mathis 1979). It is thus clear that the extinction ratios are too uncertain to be of much value in estimating this important quantity, even in the outer portions of the ρ Oph cloud (Carrasco, Strom, and Strom 1973; see below).

Having obtained the cumulative star number curves shown in Figures 3*a*–3*c*, the variation of extinction with position in the cloud was determined at each color, λ, on a spatial grid of 98″ (thus matching the spacing of the radio data—see § II*b*). This was done by dividing the cloud up into a regular grid of "reseau" squares and tallying the number of cataloged stars, n_λ, brighter than the appropriate limiting magnitude, $m_\lambda^{\rm lim}$, lying within each reseau element. (It is easily shown that in making these counts one can neglect the presence of secondary images produced by the Racine wedge.) The random error associated with the count of n_λ stars is $\pm\sqrt{n_\lambda}$; the uncertainty associated with a count of zero stars is one star, and in practice, count of $n_\lambda = 0$ are thus assigned the value 1 (Dickman 1978*b*), except as described below. By rescaling the star number $n_\lambda \rightarrow N_\lambda(m_\lambda)$ to correspond to an area of 1 deg^2, an effective apparent magnitude, m_λ, was then associated with the counted number of stars n_λ, by using the density curves in Figure 3. The difference $(m_\lambda^{\rm lim} - m_\lambda) = A_\lambda$, the extinction at color λ in the square. In matching the area-adjusted star numbers N_λ to the correct apparent magnitude, m_λ, linear interpolations of the density curves of Figure 3 were used.

Contiguous areas of the cloud empty of stars and larger than one reseau element require special treatment; clearly, such areas have, on average, larger extinctions than single, isolated reseau cells with no stars. As noted by Dickman (1978*b*), the least biased method for dealing with such regions is to assume that they possess uniform obscuration. In the region of the cloud field for which we also have radio data, there are only two such areas which required such special treatment. For example, at N band (the data set used to produce the extinctions which we ultimately compare to the ^{13}CO column densities described below), the minimum extinction in a single, isolated pixel without stars is $A_N \sim 5.6$ mag; however, by accounting for the lack of stars in adjacent pixels, the largest star-free region in the cloud field is found to have a minimum extinction $A_N \sim 9$ mag.

Studies comparing molecular column densities with dust extinction in the visible portion of the spectrum generally refer extinctions to V band. To do so, we utilize the extinction curve given by Savage and Mathis (1979). However, in order to define fully the ratios A_λ/A_V, it is also necessary to adopt a value for the ratio of total to selective extinction, R. We have noted above that our own determinations of R in the very lightly obscured cloud envelope are inconclusive, although work on the heavily obscured central regions of the ρ Oph cloud by Carrasco, Strom, and Strom (1973) suggests a value of R ~ 5–6, considerably larger than the value ~3 usually believed to characterize the diffuse interstellar medium. However, Elias (1978*a*) does not find evidence for an enhanced value of R in this region, nor does de Geus (1988). For simplicity, we have thus adopted a value of R = 3 in defining the conversions $A_\lambda \rightarrow A_V$, which are listed in the last column of Table 1. As a result, the largest visual extinctions probed by this study are at least $A_V \sim 15$ mag. If R = 5 were instead assumed, the ratio A_V/A_N, would be ~20% lower, and the largest extinctions at least $A_V \sim 12$ mag.

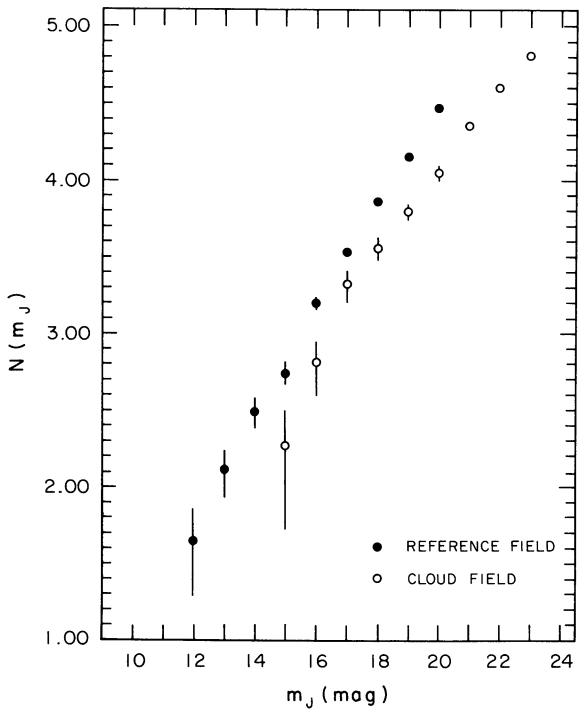

FIG. 2a

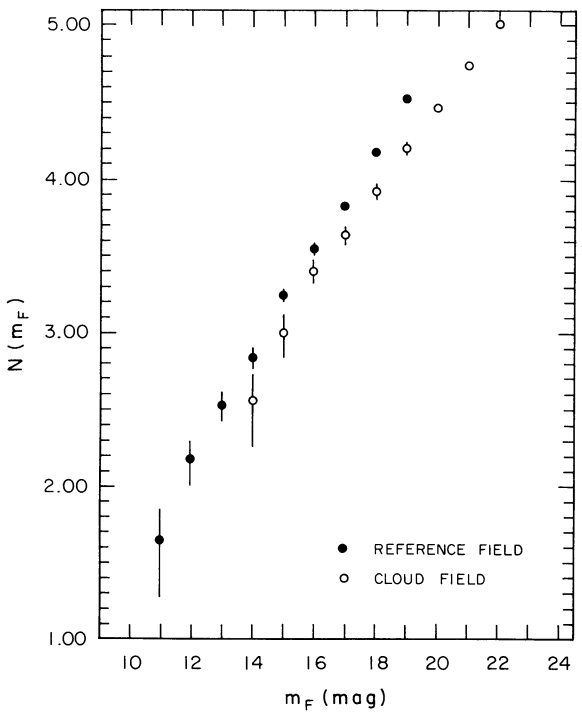

FIG. 2b

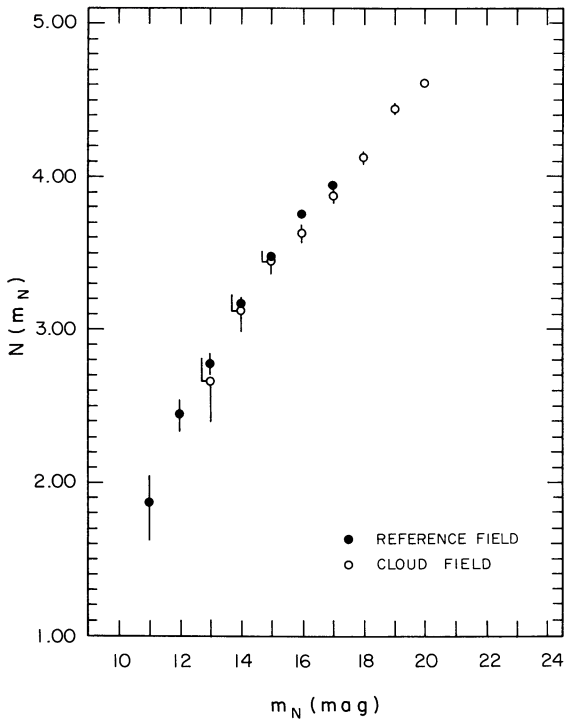

FIG. 2c

FIG. 2.—(*a–c*) Cumulative stellar surface densities in all three colors determined for both the reference field and the small region of the cloud field outlined in Fig. 1. Units are apparent magnitude (abscissa) and number of stars brighter per square degree of sky than apparent magnitude m_λ (ordinate). Error bars reflect an assumed uncertainty of $\sqrt{n}$ for a count of n stars. The differences between the cloud and reference fields are due to the presence of a small amount of extinction ($A_V \sim 1$ mag) over the small cloud area (§ II).

The map of visual extinctions over the cloud field was smoothed to a resolution of 2'.5 prior to examining the correlation of extinction and ^{13}CO column density. Not only does this reduce the random noise at high extinctions associated with statistical fluctuations in star numbers, but it also smooths the (artificially) discreet extinction values which the star count method returns when there are only one or two stars in each reseau element.

For two reasons, we shall use the extinctions based on the *N* band star counts exclusively in the remainder of this work. First and most important, the *N* band data have the longest wavelength of the three colors used in this study so that they probe the highly obscured core of the cloud most deeply. As a result, the *N* band data cover the largest range of extinctions available in this study. Second, the method of dealing with large star-free regions discussed above necessarily produces discontinuities in extinction levels which grow with the area of the regions in question. The star-free areas in the cloud at *J* and *F* (particularly *J*) are so large, that undesirably large discontinuities in the extinction range of the data result. Consequently, the *N* band star counts produce the smoothest coverage of the extinction range spanned by the cloud.

b) *Radio Data*

The radio data consist of 19 × 19 maps in the $J = 1 \rightarrow 0$ lines of the $^{12}C^{16}O$ (hereafter, CO) and $^{13}C^{16}O$ (hereafter, ^{13}CO) lines of carbon monoxide. The location of the radio grid with respect to the optical field is shown in Figure 4. The CO data were taken with the 13.7 m radio telescope of the Five College Radio Astronomy Observatory, the maps being centered at $\alpha = 16^h30^m00^s.0$, $\delta = -24°29'00''$. The map spacing of 98″ was chosen to correspond to two ^{13}CO antenna beamwidths, and the spectra were obtained with a 512 channel × 250 kHz width filter bank. This provided velocity

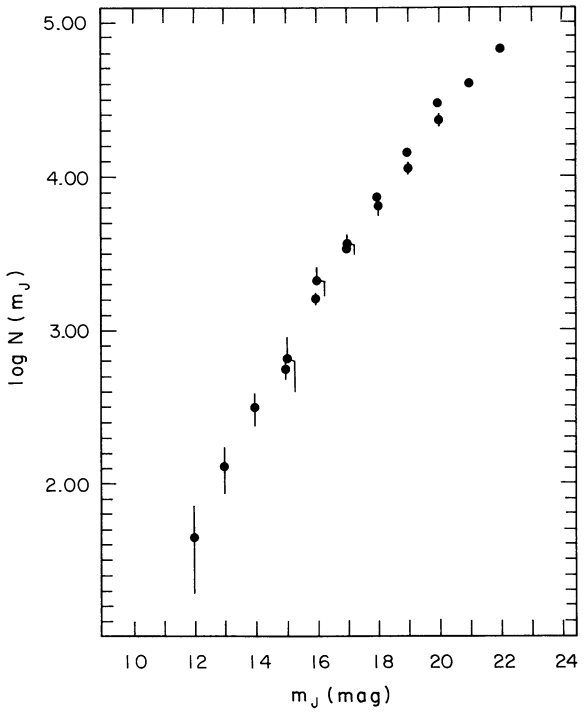

FIG. 3a

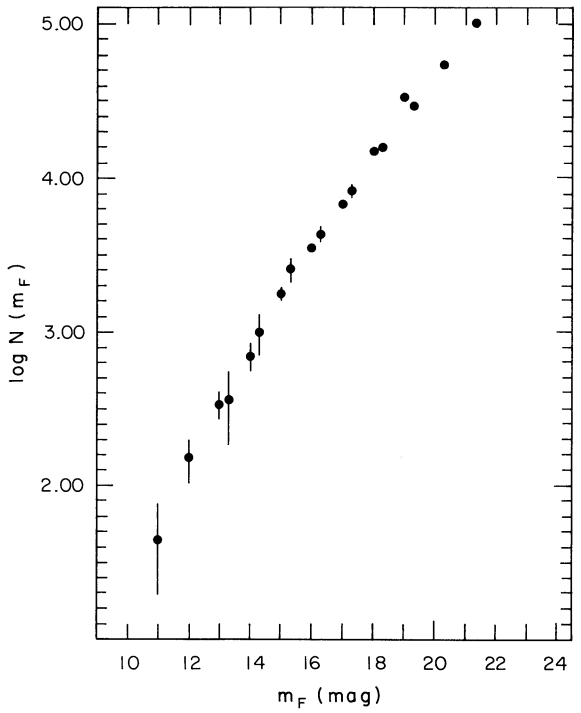

FIG. 3b

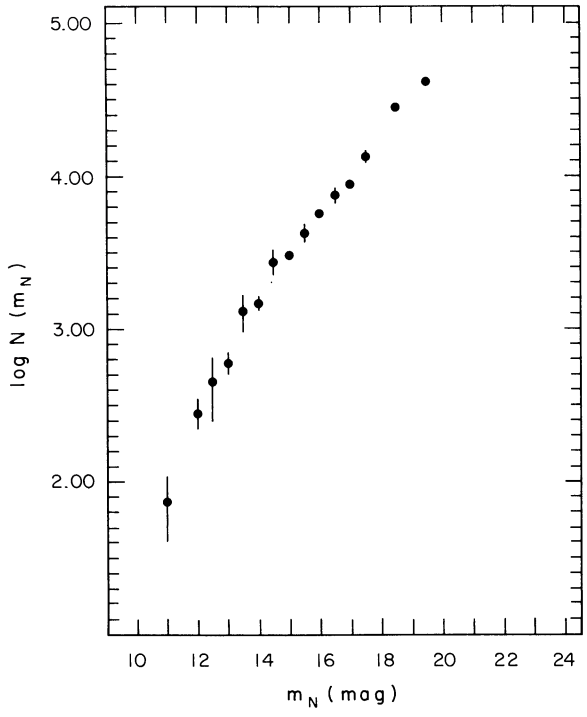

FIG. 3c

FIG. 3.—(*a–c*) Cumulative stellar surface densities in all three colors, after correcting the cloud field data for extinction. Units are identical to those used in Figs. 2*a–2c*.

resolution of 0.65 and 0.67 km s^{-1} for the CO and ^{13}CO lines, respectively. This was not always sufficient to resolve well the ^{13}CO lines, which are sometimes as narrow as $\Delta v \sim 1$ km s^{-1} (see below).

Owing to its low declination, our observations of the phiuchus cloud were restricted to an elevation range $\sim 18°$–$24°$ (where the larger value is the source elevation at transit). At such large airmasses (2.5–3.2) chopper-wheel calibrations (Penzias and Burrus 1979) were carried out before each scan, and antenna tippings made several times during each observing session were used to determine the elevation-dependent corrections (Snell and Schloerb 1983; Kenney and Taylor 1988) for atmospheric attenuation required to convert the observed antenna temperatures to radiation temperatures. At the low source elevations listed above, system temperatures referred to the top of the atmosphere were typically ~ 1000 and 2000 K, for the ^{13}CO and CO lines, respectively. Integration times ranged from 1 to 2 minutes for both isotopes, depending upon observing conditions, with typical rms noise levels $\Delta T_a \sim 0.7$ and 0.3 K, respectively.

After correcting the data to a radiation temperature scale, ^{13}CO column densities were calculated using the LTE method (Dickman 1978*a*), which assumes that both the ^{13}CO and CO $J = 1 \rightarrow 0$ lines have identical and uniform excitation temperatures along each line of sight, and that the CO line is optically thick. The typical fractional *internal* error in a measurement of LTE column density toward the heavily obscured cloud core—the region of greatest interest in the present study—is ~ 0.1–0.3, depending primarily upon the strength and width of the ^{13}CO lines (Taylor 1989); at the cloud edges where the ^{13}CO lines grow weak, the formal fractional errors are larger. However, far more serious (and unquantifiable) errors are associated with the column density measurements: the filter-channel dilution referred to above (which, since integrated intensity is conserved when a spectral line is diluted, becomes important when ^{13}CO line center optical depths exceed ~ 0.5), and the systematic errors associated with the LTE method itself.

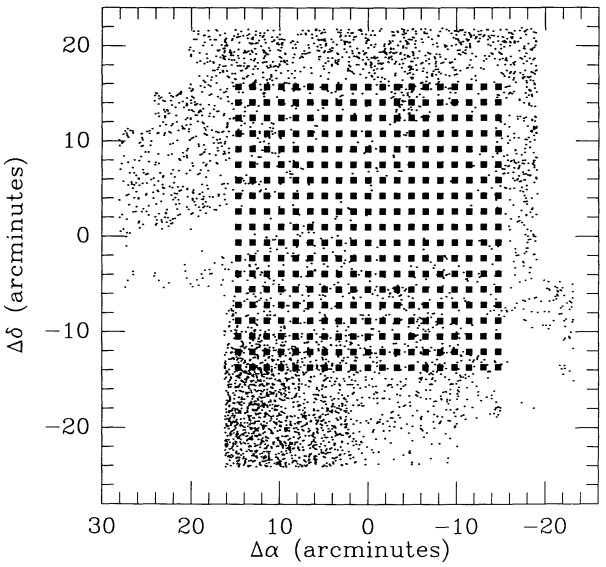

FIG. 4.—Relationship of the carbon monoxide map grid to the optical field: CO and ^{13}CO map points (*filled squares*) are superposed on the data of Fig. 1.

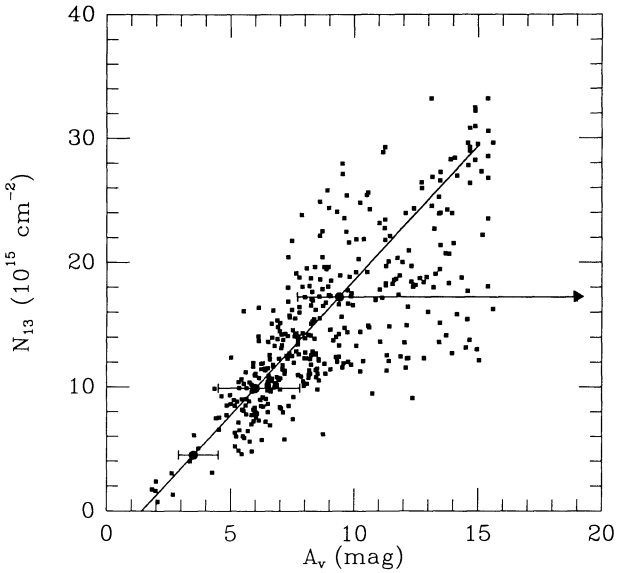

FIG. 5.—Relation of visual extinction, A_V to ^{13}CO LTE column density, N_{13}. The radio data were taken at a resolution of ~45″, spaced by 98″. The extinctions were calculated from star counts at *N*-band, as described in the text. They have been converted to *V* band assuming a ratio of total to selective extinction R = 3.1, using the extinction curve of Savage and Mathis (1979); the extinctions would be ~20% lower if a value R = 5 were used. All extinction values greater than ~10 mag should be regarded as lower limits. The extinction and ^{13}CO column density arrays were smoothed to a common resolution of ~2′.5 prior to plotting. The regression line in the figure was obtained by a least-squares fit involving only data points for which $A_V \leq 10$ mag, since systematic errors associated with the method adopted for treating large, star-free areas arise above this cutoff. Error bars arising from $\sqrt{n}$ star count fluctuations are also illustrated for the representative extinction values.

Prior to correlation with the optical data, the ^{13}CO column density map was smoothed to the same resolution as that of the visual extinction (see above).

III. RESULTS AND DISCUSSION

Figure 5 shows the relation of visual extinction to ^{13}CO LTE column density in the cloud field. Although the relationship is somewhat noisy, the two quantities are clearly correlated with one another to a high degree. A linear least-squares fit involving only points with $A_V \leq 10$ mag gives

$$N_{13}^{\rm fit} = (2.16 \pm 0.12)A_V - (3.06 \pm 0.90)\,, \qquad (2)$$

where $N_{13}^{\rm fit}$ is in units of 10^{15} cm^{-2}, and A_V is in magnitudes. The regression line given by equation (2) is also illustrated in the figure. Note that all extinctions greater than ~10 mag in the figure are lower limits and that points with extinctions greater than this value were excluded from the fit because the specific assumptions used to interpret the extinction in star-free regions larger than 1 reseau element introduce systematic errors in addition to those associated with the statistical fluctuations in star numbers. As noted above, the latter originate in the $\sqrt{n}$ error associated with a count of *n* stars, and lead to nonsymmetric errors on the extinctions, A_V. This is illustrated in Figure 5, where the error bars associated with three particular values of A_V have been plotted.

The ^{13}CO–A_V correlation is noisiest at high extinctions and column densities. The fact that internal errors in the determination of ^{13}CO column densities are lowest at high column densities where the signal to noise ratio of the data is highest (although LTE corrections for line saturation may be imperfect) suggests that the increasingly large errors associated with determining A_V at high obscuration levels play a major role in the increased scatter at high extinction seen in Figure 5.

Although we have made a formal linear fit to the data in Figure 5, it is important to avoid overinterpreting the fit. Caution is required for several reasons, including:

1. Systematic errors in the ^{13}CO column density determinations are likely to be comparable to random errors, and are very difficult to assess and include in the fit (see, for example, Taylor 1989).

2. As shown in Figure 5, $\sqrt{n}$ fluctuations in star numbers which are symmetrically distributed about a mean value, *n*, lead to highly asymmetric fluctuations in A_V which are strongly biased to very high extinctions. Consequently, at high extinctions an unweighted least-squares fit leads to a erroneously low N_{13}/A_V ratio, and over a large extinction range, spurious curvature may appear in the N_{13}/A_V plot.

3. The presence of spurious stars on the *N* band plate, images falsely identified by the densitometer's star-recognition algorithm will lower the derived extinctions. However, while the hypered IV-*N* emulsion used for the *N* band exposures is particularly prone to produce spurious, pointlike images, the very conservative magnitude limit imposed on the *N* band data should suppress both problems to negligible levels in the present work.

4. The star count method assumes that there are no foreground stars. The presence of a star lying between the Sun and the ρ Oph cloud will always lead to an erroneously low extinction as calculated by the star count method. Errors of this type are important only for the most highly obscured reseau elements, however, since in lightly obscured regions where the number of stars per unit area of sky is large, the inclusion of one or two foreground stars will affect the total number of counted stars in only a very minor way. The effect of foreground stars which lie in front of more highly obscured regions

of the cloud is more difficult to assess and depends on the stellar population lying between the Sun and the Ophiuchus cloud. As noted by Dickman and Herbst (1990), if one assumes a Wielen, Jahreiss, and Krüger (1983) field star luminosity function which continues to decline through the hydrogen-burning limit of the main sequence, only some five foreground stars are expected to lie between the Sun and the darkest portions of the ρ Oph cloud observed here; at worst, this might then affect $\sim 5\%$ of the ~ 100 high-extinction cloud pixels in this study. This is a lower limit since there are suggestions that the luminosity function may again rise at its faint end (Hawkins and Bessel 1989), and since the ρ Oph cloud itself may have produced significant numbers of dwarf stars in the past, some of which might now lie close to the edge of the cloud facing the Earth.

5. Clumpiness in the molecular cloud may allow background stars to shine through regions with large average dust column densities. Again, this effect would lead to an underestimate of the mean dust extinction. There is, in fact, increasingly compelling observational and theoretical evidence for the presence of clumping in giant molecular clouds (but not dark clouds; see summaries by, i.e., Kwan and Sanders 1987; Wilson 1989; Taylor 1989; Taylor and Dickman 1989, 1990). It is not currently known if the region of the ρ Oph cloud studied in this work is significantly clumped.

Figure 5 indicates that the correlation of ^{13}CO LTE column density and star-count based extinctions persists in the ρ Oph cloud well beyond the extinction limit of $A_V \sim 5$–6 mag usually associated with stars counts from the Palomar Sky Survey plates and similar materials. While there is an offset in A_V at which the intercept at zero column density occurs, the ratio of A_V to N_{13} given by the slope in equation (2) above, is 0.46. This is within 2 fit standard deviations of the result for the general interstellar medium given by Dickman and Clemens (1983), 0.52, and in view of the errors involved (see also Dickman 1978*a*) does not therefore differ significantly from it (although Dickman and Clemens did not treat the possible existence of an extinction offset in the data set which they analyzed). The slope of the present result also does not differ substantially from that obtained by Frerking, Langer, and Wilson (1982) for the ρ Oph region, nor from the equivalent N_{13}/A_V slope obtained by Encrenaz, Falgarone, and Lucas (1975) in their study (see summary by Bachiller and Cernicharo 1986).

We now consider the issue of the intercept of the relation shown in Figure 5. Equation (2) can be rewritten as

$$N_{13}^{\rm fit} = 2.16(A_V - 1.42) . \quad (3)$$

Thus, at least in the section of the ρ Oph cloud studied in this work, measurable ^{13}CO column densities do not occur until an extinction threshold of $A_V \sim 1.4$ mag is reached. While Encrenaz, Falgarone, and Lucas (1975) did not explicitly note the presence of an extinction threshold in their study of the ρ Oph cloud core, they state in the Appendix to their paper that the reference field used for the star counts possesses a color excess $E(B-V) = 0.27$ mag. For a ratio of total to selective extinction of $R = 3.1$, this implies an extinction of $A_V = 0.84$ mag in the reference field, an offset which is apparently not included in their extinction plots. Thus, consistent with our results here Encrenaz, Falgarone, and Lucas also found an extinction threshold of ~ 1 mag at V for the ρ Oph cloud.

Frerking, Langer, and Wilson (1982) determined a formal extinction offset of 1.6 mag in their study of the ^{13}CO to A_V ratio in the ρ Oph complex, in apparent agreement with the offset of 1.4 mag found here. However, the offset pertains only to a linear fit which they carried out over the extinction range $4 < A_V < 15$ mag, and inspection of Figure 5 of that work indicates that only undetectable or barely measurable ^{13}CO column densities are found at extinctions below $A_V \sim 4$ mag. This suggests the presence of an extinction offset much larger than the value which we obtain.

However, the extinctions in FLW were not derived from stars counts. Instead, they were taken from estimates by Elias (1978*a*) made largely on the basis of IR CO bandhead depths in background giants (which permitted a rough spectral classification), combined with IR color measurements.[1] The technique therefore yields an estimate for the total extinction in the (narrow) column of dust lying between the observer and the star. Since the stars observed by Elias are all intrinsically quite luminous and thus potentially very distant, there is the worrisome possibility that part (or all) of the extinction inferred for the background stars is not associated with the ρ Oph cloud, but arises from general interstellar reddening. If this is the case, at least some of the apparent extinction offset see in FLW's Figure 5 is spurious insofar as the issue of the $^{13}CO/A_V$ ratio in molecular clouds is concerned.

Although the spectral classifications provided by Elias (1978*a*) are quite rough, it is possible to test this hypothesis by using Elias' 1.2 μm photometry and spectral classes in combination with Johnson's (1966) standard data to estimate the distances to the background stars used as extinction probes by FLW. If we adopt a simple Galactic extinction model, with a constant in-plane gradient $\nabla_x A_V = 2$ mag kpc^{-1}, and an exponential vertical falloff with a scale height of ~ 200 pc, the general extinction suffered by a star at distance D, seen toward the ρ Oph complex ($b \sim 15°$) is

$$\Delta A_V = \int_0^D (\nabla_x A_V) \exp - \frac{l \sin b}{z_0} \cos b \, dl$$

$$= 1.5\left(1 - \exp \frac{-D}{z_0}\right) \text{mag} . \quad (4)$$

Applying the corrections indicated above to the extinctions used by FLW reduces the average visual extinction for the four lowest data points of FLW from 3.4 mag to 1.9 mag. Despite the crudeness of these estimates, we may therefore regard the extinction offset associated with FLW's study as consistent with the present work.

If we accept the presence of an extinction offset of ~ 1.5 mag in the ρ Oph region, there remains the question of the specific relationship of the dust producing this offset to the ρ Oph molecular cloud. This is particularly important given the widespread application of $^{13}CO/A_V$ ratios to determine cloud masses (e.g., Dickman 1988) and the existence of apparent extinction thresholds in CO isotope-extinction correlations for other clouds, as has been pointed out by several workers (FLW 1982; Duvert, Cernicharo, and Baudry 1986; Bachiller and Cernicharo 1986; Cernicharo and Güelin 1987; see summary by Bachiller and Cernicharo 1986). In connection with the present work, we note that de Geus (1988) has made a detailed photometric study of stars in the Scorpius-Centaurus OB association. A plot of extinction versus distance modulus for members of Upper Scorpius, the youngest subgroup associated with the ρ Oph cloud, shows no stars with extinctions exceed-

[1] FLW did attempt to use star counts to confirm the extinctions given by Elias at low A_V. However, they provide few details, and inspection of their Ophiuchus data in their Fig. 2 suggests that the confirmation is, at best, inconclusive.

ing 1 mag closer than 120 pc (the closest star in the sample is ~70 pc away). Further, the nearest star in the sample with an extinction in excess of 2 mag is 160 pc distant. These results suggest the presence of a relatively nearby, diffuse envelope beginning at a distance of ~120 pc, which is associated with the main body of the cloud at $d = 160$ pc (Elias 1978*a*), and which possesses a visual extinction consistent with the offset (1.4 mag) determined in this work. Even disregarding the issue of whether CO and ^{13}CO could be present in a region so diffuse (because of the low gas density and strongly dissociative *u-v* radiation field), the gas density is in any case too low to produce measurable molecular emission: a total extinction of 1 mag over a path length of 40 pc corresponds to a mean H_2 density of only 8 cm^{-3} (Savage and Mathis 1979), far too low to collisionally excite even CO. Consequently, the *molecular* mass of the ρ Oph cloud should be well established by simply using the *slope* of the relation above and ignoring the offset entirely. This is so provided, of course, that one is willing to accept the constancy of a particular proton column density to visual extinction ratio, such as that of Savage and Mathis (1979). This last issue is discussed in detail elsewhere (Dickman 1978*a*, 1988).

While extended envelopes may be common features of molecular clouds, simple gravitational binding arguments suggest that denser envelopes, more tightly bound than the Oph foreground material are likely to be more prevalent. Indeed, Gúelin and Cernicharo (1988) suggest that toward the Taurus clouds, a diffuse envelope produces detectable emission from the abundant CO molecule, but not from the less common ^{13}CO species (whose excitation is not assisted by photon trapping). Since low-density envelopes probably contribute most of the mass of at least the larger interstellar clouds, virial mass estimates based on the CO line should therefore be used to supplement masses for these objects computed using the ^{13}CO molecule. The existence of a severe discrepancy may indicate the presence of a diffuse envelope with H_2 densities too low to excite ^{13}CO (although these issues are not completely straightforward, as shown by Lee, Snell, and Dickman 1990).

IV. SUMMARY

We have carried out a study of the ^{13}CO–A_V relation at high visual extinctions in one section of the ρ Ophiuchi molecular cloud complex. By establishing our own calibrated stellar surface density curves, and using deep, wide-field photographic materials at $\lambda \sim 8000$ Å, our work avoids many of the difficulties ordinarily associated with using star counts to determine very high extinctions. LTE ^{13}CO column density is found to be well correlated with visual extinction on a spatial scale of ~3′ in the range $0 \leq A_V \leq 10$ mag, with a least-squares fit giving the result

$$N_{13}^{\rm fit} = (2.16 \pm 0.12)A_V - (3.06 \pm 0.90) .$$

The slope of the ^{13}CO–A_V relation is consistent with our previous work (Dickman and Clemens 1983; Dickman 1988), and with other studies of this quantity (see summary by Bachiller and Cernicharo 1986), except in the Taurus clouds (Frerking, Langer, and Wilson 1982; Cernicharo and Gúelin 1987). The nonzero intercept in the relation above indicates the existence of an extinction threshold of 1.4 mag, which must be exceeded in order for there to be observable ^{13}CO emission. We argue that de Geus' (1988) photometric work suggests an origin for the threshold in a diffuse, foreground layer of the main Ophiuchus cloud. As such, the *molecular* mass of the ρ Oph clouds should be well established by simply using the *slope* of the relation above and ignoring the offset entirely, provided that one wishes to accept the universality of a particular proton column density to extinction ratio, such as that of Savage and Mathis (1979). However, envelopes considerably denser than that of the Oph cloud are likely to be common and precautions should be taken against errors resulting from neglecting their contributions to cloud masses.

We are pleased to acknowledge the assistance of Denise Chapman-Taylor, Carolyn Jordan, and Thomas H. Jarrett in various stages of this research. R. L. D.'s work was partially supported by NSF grant AST 85-12903. This is contribution No. 702 of the Five College Astronomy Department.

REFERENCES

Bachiller, R., and Cernicharo, J. 1986, *Astr. Ap.*, **166**, 283.
Bohlin, R. C., Savage, B. D., and Drake, J. F. 1978, *Ap. J.*, **224**, 132.
Bok, B. J. 1937, *The Distribution of Stars in Space* (Chicago: University of Chicago Press).
Bok, B. J., and McCarthy, C. C. 1974, *A.J.*, **79**, 42.
Bruzual, G. A. 1966, Ph.D. thesis, University of California, Berkeley.
Carrasco, L., Strom, S. E., and Strom, K. M. 1973, *Ap. J.*, **182**, 95.
Cernicharo, J., and Gúelin, M. 1987, *Astr. Ap.*, **176**, 299.
de Geus, E. 1988, Ph.D. thesis, University of Leiden.
Dickman, R. L. 1978*a*, *Ap. J. Suppl.*, **37**, 407.
———. 1978*b*, *A.J.*, **83**, 363.
———. 1988, in *Molecular Clouds in the Milky Way and External Galaxies*, ed. R. L. Dickman, R. L. Snell, and J. S. Young (Berlin: Springer-Verlag), p. 55.
Dickman, R. L., and Clemens, D. P. 1983, *Ap. J.*, **271**, 143.
Dickman, R. L., and Herbst, W. 1990, in preparation.
Duvert, G., Gernicharo, J., and Baudry, A. 1985, *Astr. Ap.*, **164**, 2.
Elias, J. E. 1978*a*, *Ap. J.*, **224**, 453.
———. 1978*b*, *Ap. J.*, **224**, 857.
Elmegreen, D. M., and Elmegreen, B. G. 1979, *A.J.*, **84**, 615.
Encrenaz, P. J., Falgarone, E., and Lucas, R. 1975, *Astr. Ap.*, **44**, 73.
Fernie, J. D. 1983, *Pub. A.S.P.*, **95**, 782.
Frerking, M. A., Langer, W. D., and Wilson, R. W. 1982, *Ap. J.*, **262**, 590 (FLW).
Gúelin, M., and Cernicharo, J. 1988, in *Molecular Clouds in the Milky Way and External Galaxies*, ed. R. L. Dickman, R. L. Snell, and J. S. Young (Berlin: Springer-Verlag), p. 81.
Harris, A. I., Stutzki, J., Herman, J., Genzel, R., Jaffe, D. T., Lugten, J. B., Stacey, G. J., and Townes, C. H. 1988, in *Molecular Clouds in the Milky Way and External Galaxies*, ed. R. L. Dickman, R. L. Snell, and J. S. Young (Berlin: Springer-Verlag), p. 195.
Hawkins, M. R. S., and Bessell, M. S. 1989, *M.N.R.A.S.*, submitted.
Johnson, H. L. 1966, *Ann. Rev. Astr. Ap.*, **4**, 193.
Kenney, J. D., and Taylor, D. K. 1988, *FCRAO Tech. Rep.*, No. 323, unpublished.
Kron, R. G. 1980, *Ap. J. Suppl.*, **43**, 314.
Kwan, J., and Sanders, D. B. 1986, *Ap. J.*, **309**, 783.
Lee, Y., Snell, R. L., and Dickman, R. L. 1990, *Ap. J.*, in press.
Lilley, A. E. 1955, *Ap. J.*, **121**, 559.
Matsakis, D. N., Hjalmarson, Å, Palmer, P., Cheung, A. C., and Townes, C. H. 1981, *Ap. J. (Letters)*, **250**, L85.
Migenes, V., Johnston, K. J., Pauls, T. A., and Wilson, T. L. 1990, *Ap. J.*, submitted.
Penzias, A. A., and Burrus, C. A., 1979, *Ann. Rev. Astr. Ap.*, **11**, 51.
Savage, B. D., and Mathis, J. S. 1979, *Ann. Rev. Astr. Ap.*, **17**, 73.
Snell, R. L., and Schloerb, F. P. 1983, *FCRAO Tech. Memo.*, unpublished.
Taylor, D. K. 1989, Ph.D. thesis, University of Massachusetts.
Taylor, D. K., and Dickman, R. L. 1989, *Ap. J.*, **341**, 293.
———. 1990, in preparation.
Tucker, K. D., Dickman, R. L., Encrenaz, P. J., and Kutner, M. L. 1976, *Ap. J.*, **210**, 679.
Wielen, R., Jahreiss, H., and Krüger, R. 1983, in *IAU Colloquium 76, The Nearby Stars and the Stellar Luminosity Function*, ed. A. G. D. Philip and A. R. Upgren (Schenectady: L. Davis), p. 163.
Wilson, T. L. 1989, preprint.

ROBERT L. DICKMAN: Radio Astronomy, LGRT, University of Massachusetts, Amherst, MA 01003

WILLIAM HERBST: Van Vleck Observatory, Wesleyan University, Middletown, CT 06457